Eur. Phys. J. A **5**, 399–408 (1999)

THE EUROPEAN PHYSICAL JOURNAL A

The structure of ^{99}Ru from (α,3n) reaction

J. Mrázek[1], M.Honusek[1], A. Špalek[1], J. Bielčík[1], J. Slívová[1], J. Adam[1], A.A. Pasternak[2]

[1] Nuclear Physics Institute, Academy of Sciences of the Czech Republic, Řež near Prague, Czech Republic
(e-mail: honusek@ujf.cas.cz)
[2] Physical–Technical Institute "A.F. Joffe", Cyclotron Laboratory, ul. Politechnitscheskaja 26, 194021 St. Petersburg, Russia

Received: 13 January 1999 / Revised version: 26 March 1999
Communicated by D. Schwalm

Abstract. The results of in-beam investigations of excited states of ^{99}Ru using the ^{98}Mo(α, 3n) reaction are presented. Angular distributions of γ–rays and γ–γ coincidences have been measured. Excited states have been identified up to an energy of E = 5603 keV and spin of $I^{\pi} = 31/2^{-}$. Mean lifetimes τ have been determined using the DSA method for eleven levels. Aligned angular momenta are discussed and the probable ($\nu h_{11/2}$) origin of a backbending at frequency about 0.5 MeV was confirmed. The possible role of ($\nu d_{5/2}$) alignment at frequencies above 0.5 MeV was pointed out.

PACS. 27.60.+j Properties of specific nuclei listed by mass ranges 90≤A≤149 – 23.20.Lv Gamma transitions and level energies – 23.20.Ck Lifetimes and transition probabilities – 23.20.En Angular distribution and correlation measurements

1 Introduction

A new region of deformation was observed in the early seventies around mass A ∼ 100. Further research revealed that different types of deformations are possible. Moreover it was determined that shape coexistence may occur [1]. An abrupt transition from spherical to deformed shape was observed for nuclei with Z ∼ 40. The presence of parent ($\pi g_{9/2}$) and ($\nu g_{7/2}$) shells accentuate the importance of the np interaction [2].

The IBA (Interacting Boson Approximation) model description was extensively used for Ru isotopes due to its ability to describe transitional nuclei. A transition from a spherical shape to a γ–unstable structure was found for these nuclei [3–5]. A similar behaviour was found in [6], where particular data for Ru isotopes with A=98–108 were studied in the ECQ (Extended Consistent Q) formalism and results were presented within Casten's triangle. A recession from vibrational character with increasing N was found for the isotopes. The "geometrical" general collective model (GCM) was also applied to Ru isotopes [1] with A=96–108 and two energy minima, spherical and triaxial at (β,γ)∼(0.4,24°), were obtained for isotopes with A≥100. The only spherical minimum was found for isotopes with A<100.

A smaller deformation of $\beta \sim 0.2$ and γ–softness were found for ^{100}Ru by spin diabatic surfaces (SDS) and total Routhian surfaces (TRS) calculations in [7].

Although the IBA-1 version of the model is not able to describe triaxial deformations, the common features in IBA-1 and GCM model results [1,5,6] – spherical shape for ^{98}Ru and development of β–deformation for the heavier Ru isotopes – were found.

Contradictions concerning γ–deformation appear in comparison of results of GCM model for Hg isotopes [1] (subjected to study in the same work as Ru isotopes) with microscopic model calculations of Bengtsson et al. [8], while results on β–deformation remain consistent.

The spin alignment was studied in [7,9] and its ($\nu h_{11/2}$) origin was shown to be responsible for the backbending at a frequency of about 0.5 MeV. Also ($\pi g_{9/2}$) origin was suggested for the backbending of ^{99}Ru at negative parity [7].

We studied [6] the isotopes ^{99,100,101}Ru in the reactions ^{98,100}Mo(α, xn). Partial results concerning the isotopes ^{100,101}Ru were published in [10]. In this paper we present our results concerning ^{99}Ru.

2 Experimental setup

The measurements were performed with a beam from the 120 cm U120M cyclotron of NPI in Řež near Prague. A target of ^{98}Mo (97% enriched) 5 mg/cm^2 thick was bombarded by 38 MeV α-particles. The experiments involved γ–γ coincidence and angular distribution measurements of γ–rays.

Gamma–gamma coincidence measurements were performed using Ge(Li) (resolution 2.7 keV at 1.3 MeV and efficiency 12 %) and HPGe (resolution 1.85 keV at 1.3 MeV and efficiency 20 %) detectors placed at 90° to the beam direction and to each other. Data were stored

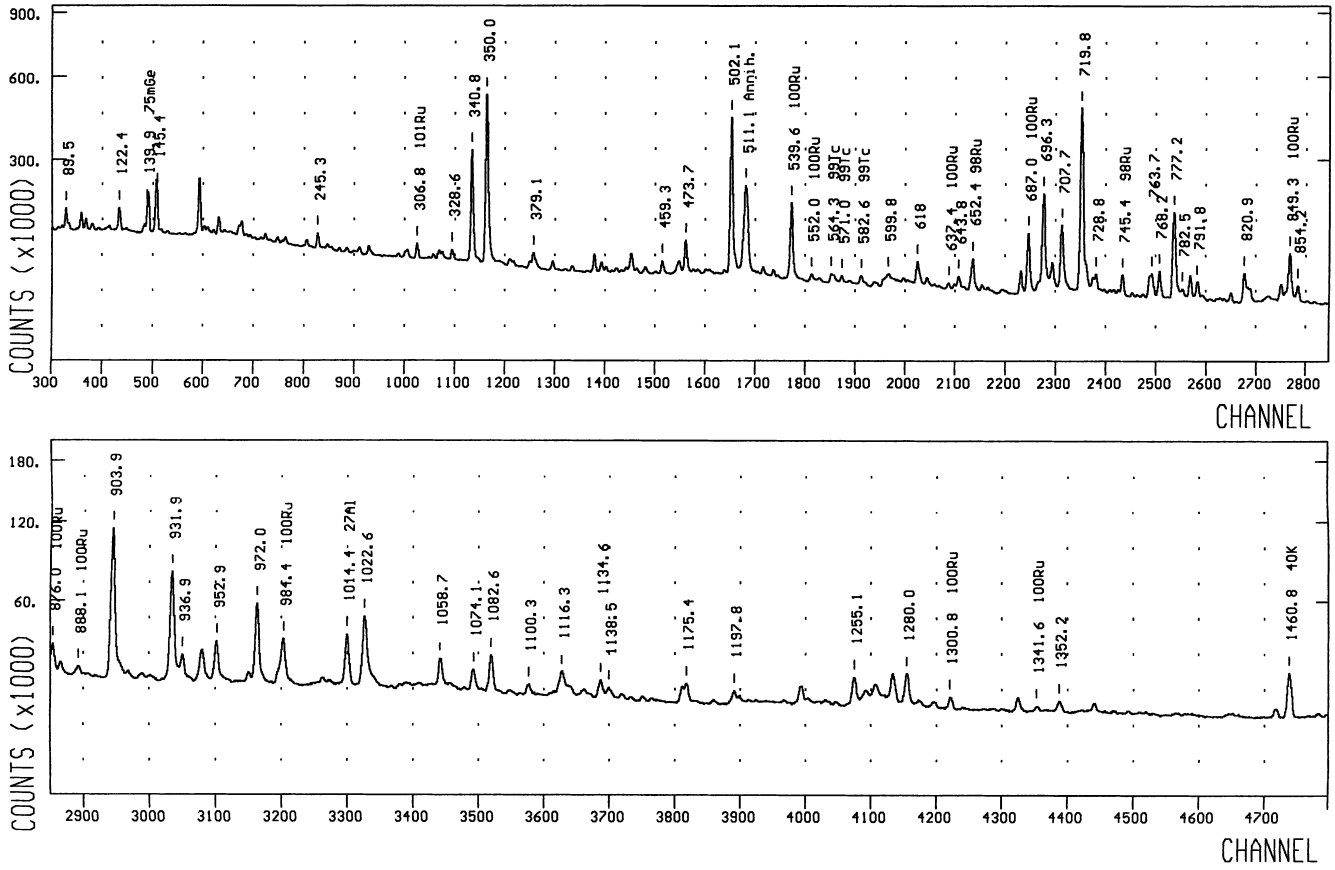

Fig. 1. A part of gamma–ray spectrum obtained from the bombardment of an enriched ^{98}Mo target with 38 MeV α–particles. Detector was positioned at 30° with respect to the beam axis

event by event for subsequent off-line analysis. Almost 7.9 $\times$ 10^8 events were taken during the measurement of γ–γ coincidences.

Angular distributions were measured using the HPGe detector at four angles θ = 30°, 55°, 90°, and 150° with respect to the beam axis.

An example of γ–ray spectra measured at 30° is shown in Fig. 1, an example of γ–γ coincidences spectra is shown in Fig. 2. All γ–ray spectra were processed using a peak fitting program DEIMOS [11].

3 Data evaluation

3.1 Angular distributions

Experimental angular distributions of γ–rays were treated using a formula [12]

$$W(\theta) \sim 1 + a_2 Q_2 P_2(\cos\theta) + a_4 Q_4 P_4(\cos\theta), \qquad (1)$$

where a_2, a_4 are experimental angular distribution coefficients, Q_2, Q_4 are detector solid angle corrections and $P_2(\cos\theta)$, $P_4(\cos\theta)$ are Legendre polynomials.

Spectra from angular distribution measurements were normalized by virtue of assumed a_2 coefficient value of the strong, well known ([13–15]) E2 transition 719.8 keV in ^{99}Ru. The a_2 coefficient value was determined using a smooth dependence of attenuation factors α_2 on spin I, obtained in ^{100}Mo(α, xn)^{100,101}Ru experiment [10]. A normalization in 100, 101Ru was based on an isomeric transition. The α_2 attenuation coefficient changes from 0.41 for spin 5/2, through 0.64 for spin 13/2, to 0.81 for spin value 31/2.

Coefficients a_2 and a_4 determined in the experiment were compared to calculated coefficients (with an assumption about spin values of initial and final levels I_i and I_f) for various values of mixing ratio δ and thus possible values of mixing ratio δ were determined. Mixing ratio is defined by

$$\delta = \frac{\langle I_f \,||\, L+1 \,||\, I_i \rangle}{\langle I_f \,||\, L \,||\, I_i \rangle}, \qquad (2)$$

where $\langle I_f \,||\, L \,||\, I_i \rangle$ is reduced matrix element between final I_f and initial I_i states and L stands for a multipolarity L transition operator [12].

3.2 Level lifetimes evaluation

Level lifetimes in range of *ps* were deduced using the Doppler Shift Attenuation (DSA) method [16] from the spectra obtained in angular distribution measurements. The program package SHAPE [16,17], which performs

Table 1. Energies, relative intensities, a_2, a_4 and δ coefficients of ^{99}Ru transitions

E_γ [keV]	I_γ	a_2	a_4	E_i [keV]	$I_i^{\pi_i} \rightarrow I_f^{\pi_f}$	δ	a^a_{2eval}
89.50(20)[b]	2.03(7)	0.105(22)	0.02(5)	89.5	$3/2^+ \rightarrow 5/2^+$	$-0.8^{+0.5}_{-0.9}$	
102.00(20)[b]	1.24(6)	-0.25(4)	-0.04(11)	719.9	$9/2^+ \rightarrow 7/2^+$	$-4.2^{+0.7}_{-0.9}$	
						-0.06 ± 0.04	
122.44(10)	2.70(11)	-0.14(4)	0.06(9)	2874.6	$19/2^+ \rightarrow 17/2^+$	$0.5^{+0.3}_{-0.25}$	
					$17/2^+ \rightarrow 17/2^+$	$-1.25^{+0.17}_{-0.2}$	
						$3.8^{+1.6}_{-0.8}$	
145.45(10)	8.5(4)	-0.28(5)	0.08(10)	3020.0	$21/2^+ \rightarrow 19/2^+$	$-7.3^{+1.5}_{-2.5}$	
						-0.04 ± 0.04	
					$19/2^+ \rightarrow 19/2^+$	$< -2; > 13$	
175.12(10)	1.02(6)	-0.16(8)	-0.07(15)	2997.5	$19/2^+ \rightarrow 21/2^+$	0.01 ± 0.06	
						< -15	
					$19/2^+ \rightarrow 19/2^+$	$-1.4^{+0.4}_{-0.8}$	
						> 2.5	
					$19/2^+ \rightarrow 17/2^+$	< -8	
						0.04 ± 0.06	
177.32(10)	0.87(4)	-0.12(5)	0.02(11)	1497.1	$13/2^+ \rightarrow 11/2^+$	$0.055^{+0.05}_{-0.04}$	
						< -9	
245.31(10)	2.89(18)	-0.26(7)	-0.08(16)	2997.5	$19/2 \rightarrow 17/2$	7^{+2}_{-4}	
						-0.04 ± 0.05	
					$17/2^+ \rightarrow 17/2^+$	$< -1.6; > 7$	
271.07(10)	0.99(12)	0.05(22)	0.2(4)	1319.7	$11/2^+ \rightarrow 11/2^+$	$-0.5^{+0.5}_{-0.8}$	
						> 0.75	
277.01(10)	1.39(5)	0.10(4)	0.07(7)	617.9	$7/2^+ \rightarrow 7/2^+$	-0.28 ± 0.09	
						$2^{+0.5}_{-0.4}$	
328.57(10)	2.05(12)	-0.19(8)	0.04(17)	1048.5	$11/2^+ \rightarrow 9/2^+$	0.0 ± 0.07	
						-6.7^{+2}_{-5}	
340.81(10)	36.2(17)	-0.27(4)	0.03(10)	340.9	$7/2^+ \rightarrow 5/2^+$	-0.1 ± 0.06	
						-3.2 ± 0.6	
350.01(10)	65.(4)	-0.24(6)	0.09(12)	1069.9	$11/2^- \rightarrow 9/2^+$	-0.04 ± 0.06	
						-5.7 ± 1.5	
351.48(20)	4.7(10)	-0.1(4)		2752.2	$17/2^+ \rightarrow 17/2^+$	$-1; 2.5$	
					$17/2^+ \rightarrow 15/2^+$	0.1 ± 0.3	
						$< -3; > 3$	
379.07(10)	2.88(11)	0.18(4)	0.02(7)	719.9	$9/2^+ \rightarrow 7/2^+$	0.35 ± 0.05	
						6.5 ± 1.5	
380.81(10)	1.37(13)	-0.06(14)	-0.06(26)	2400.9	$17/2^+ \rightarrow 15/2^+$	$\lvert\delta\rvert > 10$	
						0.1 ± 0.1	
					$15/2^+ \rightarrow 15/2^+$	$-0.9^{+0.4}_{-0.7}$	
						$2.6^{+8}_{-1.1}$	
421.27(10)	1.85(6)	0.23(4)	-0.02(6)	2822.3	$21/2^+ \rightarrow 17/2^+$		0.306 ± 0.015
					$19/2^+ \rightarrow 17/2^+$	$0.32^{+0.04}_{-0.03}$	
						$4.7^{+0.8}_{-0.6}$	
					$17/2^+ \rightarrow 17/2^+$	-0.29 ± 0.07	
448.59(10)	1.53(9)	0.13(8)	0.02(15)	1497.1	$13/2^+ \rightarrow 11/2^+$	0.26 ± 0.07	
						> 5.2	
459.26(10)	2.89(13)	0.09(6)	0.00(11)	2852.0	$19/2^+ \rightarrow 17/2^+$	0.22 ± 0.45	
						$9^{+5}_{-2.5}$	
					$17/2^+ \rightarrow 17/2^+$	-0.57 ± 0.12	
						1.4 ± 0.3	
468.26(10)	1.35(7)	0.07(7)	-0.25(11)	2330.0	$13/2^- \rightarrow 13/2^-$	-0.54 ± 0.16	
						$1.6^{+0.6}_{-0.4}$	
					$15/2^- \rightarrow 13/2^-$	$0.2^{+0.7}_{-0.6}$	
						> 7	

Table 1. (continued)

E_γ [keV]	I_γ	a_2	a_4	E_i [keV]	$I_i^{\pi_i} \rightarrow I_f^{\pi_f}$	δ	a^a_{2eval}
473.67(10)	10.8(4)	-0.311(28)	0.01(6)	2874.6	$19/2^+ \rightarrow 17/2^+$	-6 ± 0.9	
						$-0.07^{+0.03}_{-0.025}$	
					$17/2^+ \rightarrow 17/2^+$	$\times$	
					$17/2^+ \rightarrow 15/2^+$	$-5.4^{+0.6}_{-0.8}$	
						$_{-0.08} \pm 0.25$	
					$15/2^+ \rightarrow 15/2^+$	$\times$	
502.07(10)	56.5(16)	0.312(18)	-0.05(3)	1571.9	$15/2^- \rightarrow 11/2^-$		0.291 ± 0.010
521.90(10)	1.55(17)	0.22(18)		2852.0	$19/2^- \rightarrow 15/2^-$		0.302 ± 0.011
					$17/2^- \rightarrow 15/2^-$	$0.32^{+0.2}_{-0.15}$	
						$4.8^{+10}_{-2.3}$	
528.36(10)	1.41(8)	0.10(7)	-0.14(14)	617.9	$7/2^+ \rightarrow 3/2^+$		0.250 ± 0.020
531.01(10)	0.320(26)	0.36(14)	-0.01(25)	2392.7	$17/2^- \rightarrow 13/2^-$		0.294 ± 0.010
					$15/2^- \rightarrow 13/2^-$	$0.47^{+0.23}_{-0.15}$	
						$3^{+2}_{-1.1}$	
596.95(15)	2.1(4)	-0.4(3)		2997.5	$19/2^- \rightarrow 17/2^-$	$-4.5^{+2.6}_{-10}$	
						$-0.12^{+0.23}_{-0.29}$	
					$17/2^- \rightarrow 17/2^-$	$< -1; > 2.5$	
599.84(10)	4.9(10)	-0.5(3)	0.2(7)	1319.7	$11/2^+ \rightarrow 9/2^+$	$-0.27^{+0.27}_{-0.5}$	
						$-2.2^{+1.4}_{-5}$	
617.89(15)[c]	7.(3)			617.9	$7/2^+ \rightarrow 5/2^+$		
617.94(25)[c]	2.5(15)			3638.2			
618.75(25)[c]	3.0(20)			3020.0			
643.76(10)	3.42(16)	0.43(7)	-0.08(11)	3036.5	$21/2^- \rightarrow 17/2^-$		0.306 ± 0.015
					$19/2^- \rightarrow 17/2^-$	$0.53^{+0.11}_{-0.09}$	
						$2.5^{+0.6}_{-0.5}$	
					$17/2^- \rightarrow 17/2^-$	0.22 ± 0.15	
650.91(25)[f]	2.01(14)	0.11(11)		2874.6	$19/2^+ \rightarrow 15/2^+$		0.302 ± 0.011
					$17/2^+ \rightarrow 15/2^+$	$0.23^{+0.1}_{-0.08}$	
						> 5	
660.01(15)	0.54(5)	-0.06(15)		1277.9	$9/2^+ \rightarrow 7/2^+$	0.11 ± 0.14	
						< -5	
661.76(15)	1.26(10)	-0.15(13)		3536.3	$21/2 \rightarrow 19/2^+$	< -7	
						0.04 ± 0.09	
					$19/2 \rightarrow 19/2^+$	$-1.4^{+0.5}_{-20}$	
						$3.9^{+6}_{-1.9}$	
682.22(10)	5.5(3)	0.30(8)	-0.15(14)	3534.2	$21/2^+ \rightarrow 17/2^+$		0.306 ± 0.015
696.33(10)	37.9(10)	0.279(14)	-0.044(26)	2268.3	$19/2^- \rightarrow 15/2^-$		0.302 ± 0.011
701.0(3)[c]	1.6(4)			2020.3	$15/2^+ \rightarrow 11/2^+$		
701.70(20)[c]	5.3(7)	0.17(8)[d]	0.02(14)	1319.7	$11/2^+ \rightarrow 7/2^+$		0.273 ± 0.009
707.56(10)	21.5(6)	0.276(17)	-0.08(3)	1048.5	$11/2^+ \rightarrow 7/2^+$		0.273 ± 0.009
719.81(10)[e]	100.0(26)	0.260(14)	-0.062(26)	719.9	$9/2^+ \rightarrow 5/2^+$		0.262 ± 0.012
728.82(10)	3.8(5)	0.38(23)	0.1(5)	1069.9	$11/2^- \rightarrow 7/2^+$		
731.7(3)	0.5(3)			2752.2	$15, 17/2^+ \rightarrow 15/2^+$		
742.70(10)	1.46(13)	-0.35(12)		4380.9	$23/2^+ \rightarrow 21/2^+$	-0.09 ± 0.09	
						-5.6^{+2}_{-5}	
					$21/2^+ \rightarrow 21/2^+$	< -2	
						> 8	
763.73(10)	6.4(3)	0.34(7)	-0.21(11)	3638.2	$23/2^+ \rightarrow 19/2^+$		0.307 ± 0.020
					$21/2^+ \rightarrow 19/2^+$	$0.42^{+0.08}_{-0.06}$	
						$3.2^{+0.8}_{-0.6}$	
					$19/2^+ \rightarrow 19/2^+$	0.2 ± 0.5	
768.19(10)	8.8(4)	0.50(7)	0.15(11)	3036.5	$21/2^- \rightarrow 19/2^-$	$0.6^{+0.17}_{-0.1}$	
						2 ± 0.5	
					$19/2^- \rightarrow 19/2^-$	$\times$	
					$17/2^- \rightarrow 19/2^-$	-1 ± 0.4	
777.25(10)	34.0(14)	0.24(4)	-0.08(8)	1497.1	$13/2^+ \rightarrow 9/2^+$		0.281 ± 0.010

Table 1. (continued)

E_γ [keV]	I_γ	a_2	a_4	E_i [keV]	$I_i^{\pi_i} \rightarrow I_f^{\pi_f}$	δ	a^a_{2eval}
782.48(10)	2.17(13)	-0.01(14)	0.01(12)	5005.3	$29/2^- \rightarrow 27/2^-$	0.13 ± 0.1	
						> 7	
					$27/2^- \rightarrow 27/2^-$	$-0.9^{+0.3}_{-0.5}$	
						$1.6^{+1.3}_{-0.6}$	
791.8(3)[c]	0.8(5)			2653.5	$\rightarrow 13/2^-$		
791.83(20)[c]	3.6(7)	0.28(4)[d]	0.08(6)	1861.7	$13/2^- \rightarrow 11/2^-$	0.41 ± 0.04	
						3.9 ± 0.6	
820.86(10)	8.23(24)	0.348(20)	0.07(4)	2392.7	$17/2^- \rightarrow 15/2^-$	0.045 ± 0.03	
					$15/2^- \rightarrow 15/2^-$	$0.04^{+0.2}_{-0.08}$	
						$0.45^{+0.1}_{-0.2}$	
846.63(10)	2.53(9)	0.28(3)	-0.02(6)	4046.8	$25/2^- \rightarrow 23/2^-$	0.35 ± 0.035	
						$4^{+0.55}_{-0.45}$	
					$23/2^- \rightarrow 23/2^-$	$-0.28^{+0.09}_{-0.08}$	
						0.67 ± 0.12	
854.18(10)	4.61(14)	0.302(21)	-0.14(4)	2874.6	$19/2^+ \rightarrow 15/2^+$		0.302 ± 0.011
					$17/2^+ \rightarrow 15/2^+$	0.4 ± 0.03	
						$3.6^{+0.3}_{-0.26}$	
903.91(15)[c]	24.0(20)	0.23(3)[d]	-0.01(6)	2400.9	$17/2^+ \rightarrow 13/2^+$		0.294 ± 0.010
					$15/2^+ \rightarrow 13/2^+$	$0.341^{+0.04}_{-0.03}$	
						$4.6^{+0.7}_{-0.6}$	
904.30(25)[c]	2.5(10)			2223.9	$13, 15/2^+ \rightarrow 11/2^+$		
931.89(10)	21.0(10)	0.36(7)	-0.10(11)	3200.2	$23/2^- \rightarrow 19/2^-$		0.307 ± 0.020
936.95(10)	2.3(6)	0.0(6)		1277.9	$9/2^+ \rightarrow 7/2^+$		
945.2(3)	1.89(16)	0.45(16)	-0.18(25)	5168.0	$29/2^- \rightarrow 27/2^-$	$0.51^{+0.4}_{-0.17}$	
						$2.4^{+1.5}_{-1.1}$	
					$27/2^- \rightarrow 27/2^-$	0.14 ± 0.5	
946.2(3)	4.06(13)	0.40(3)	-0.16(5)	3982.7	$25/2^- \rightarrow 21/2^-$		0.312 ± 0.024
					$23/2^- \rightarrow 21/2^-$	0.48 ± 0.05	
						$2.7^{+0.4}_{-0.3}$	
					$21/2^- \rightarrow 21/2^-$	0.18 ± 0.22	
952.87(10)	6.7(3)	0.41(7)	-0.07(11)	4487.0	$27/2^- \rightarrow 23/2^-$		0.31 ± 0.03
971.95(10)	12.3(3)	0.308(17)	-0.05(3)	2020.3	$15/2^+ \rightarrow 11/2^+$		0.291 ± 0.010
1022.62(20)[f]	11.7(6)	0.27(6)	-0.14(11)	4222.8	$27/2^- \rightarrow 23/2^-$		0.31 ± 0.03
1058.7(3)[c]	0.8(5)			4518.3			
1058.7(3)[c]	4.4(7)	0.11(7)[d]		3459.6	$\rightarrow 15, 17/2^+$		
1070.03(10)	0.5(3)	-0.2(12)		1069.9	$11/2^- \rightarrow 5/2^+$		
1074.14(10)	2.82(21)	0.30(13)	-0.06(22)	3094.5	$19/2^+ \rightarrow 15/2^+$		0.302 ± 0.011
					$17/2^+ \rightarrow 15/2^+$	$0.4^{+0.17}_{-0.12}$	
						$3.6^{+2.6}_{-1.3}$	
1082.56(10)[f]	6.04(28)	0.33(6)	-0.20(11)	4102.6	$25/2^+ \rightarrow 21/2^+$		0.312 ± 0.024
					$23/2^+ \rightarrow 21/2^+$	0.4 ± 0.07	
						$3.3^{+0.8}_{-0.6}$	
					$21/2^+ \rightarrow 21/2^+$	$-0.15^{+0.3}_{-0.15}$	
						$0.6^{+0.2}_{-0.4}$	
1100.34(10)	1.56(14)	0.16(16)	-0.19(29)	3324.3	$19/2 \rightarrow 15/2^+$		0.302 ± 0.011
					$17/2^+ \rightarrow 15/2^+$	$0.27^{+0.16}_{-0.13}$	
						6^{+20}_{-3}	
1116.30(20)[f]	4.3(10)	0.2(5)	0.0(9)	5603.3	$31/2^- \rightarrow 27/2^-$		0.32 ± 0.04
1134.55(10)	2.32(11)	0.31(6)	-0.42(11)	5357.3	$31/2^- \rightarrow 27/2^-$		0.32 ± 0.04
1138.49(10)	1.05(13)	0.28(26)		4232.9	$23/2^+ \rightarrow 19/2^+$		0.307 ± 0.020
					$21/2^+ \rightarrow 19/2^+$	$0.36^{+0.4}_{-0.2}$	
						4^{+20}_{-2}	
1175.45(10)	2.49(9)	0.25(3)	-0.03(6)	2223.9	$15/2^+ \rightarrow 11/2^+$		0.291 ± 0.010
					$13/2^+ \rightarrow 11/2^+$	$0.37^{+0.5}_{-0.4}$	

Table 1. (continued)

E_γ [keV]	I_γ	a_2	a_4	E_i [keV]	$I_i^{\pi_i} \rightarrow I_f^{\pi_f}$	δ	a^a_{2eval}
1197.76(20)	1.87(9)	0.51(7)	0.07(11)	3466.0	$23/2^- \rightarrow 19/2^-$		0.307 ± 0.020
					$21/2^- \rightarrow 19/2^-$	$0.63^{+0.2}_{-0.11}$	
						2 ± 0.5	
					$19/2^- \rightarrow 19/2^-$	$\times$	
1255.08(10)	4.3(3)	0.24(13)	-0.28(23)	2752.2	$17/2^+ \rightarrow 13/2^+$		0.294 ± 0.010
					$15/2^+ \rightarrow 13/2^+$	$0.35^{+0.15}_{-0.12}$	
						$4.5^{+4}_{-1.7}$	
1280.00(10)	5.0(4)	0.36(12)	0.06(20)	2852.0	$19/2^- \rightarrow 15/2^-$		0.302 ± 0.011
					$17/2^- \rightarrow 15/2^-$	$0.46^{+0.18}_{-0.13}$	
						$3^{+1.6}_{-1}$	
1352.18(10)	1.57(11)	0.18(12)	0.15(21)	2400.9	$17/2^+ \rightarrow 11/2^+$		
					$15/2^+ \rightarrow 11/2^+$		0.291 ± 0.010

[a] calculated values of a_2 (a_{2eval}) are presented in the last column for E2 transitions to enable comparison with the experimental a_2 value (see text)
[b] transition was not observed in coincidence spectra because of its low energy
[c] peak is a part of unresolved multiplet, I_γ is deduced from coincidences
[d] a_2 and a_4 are values for multiplet
[e] transition 719.8 keV was used for angular distribution normalization
[f] possible doublet

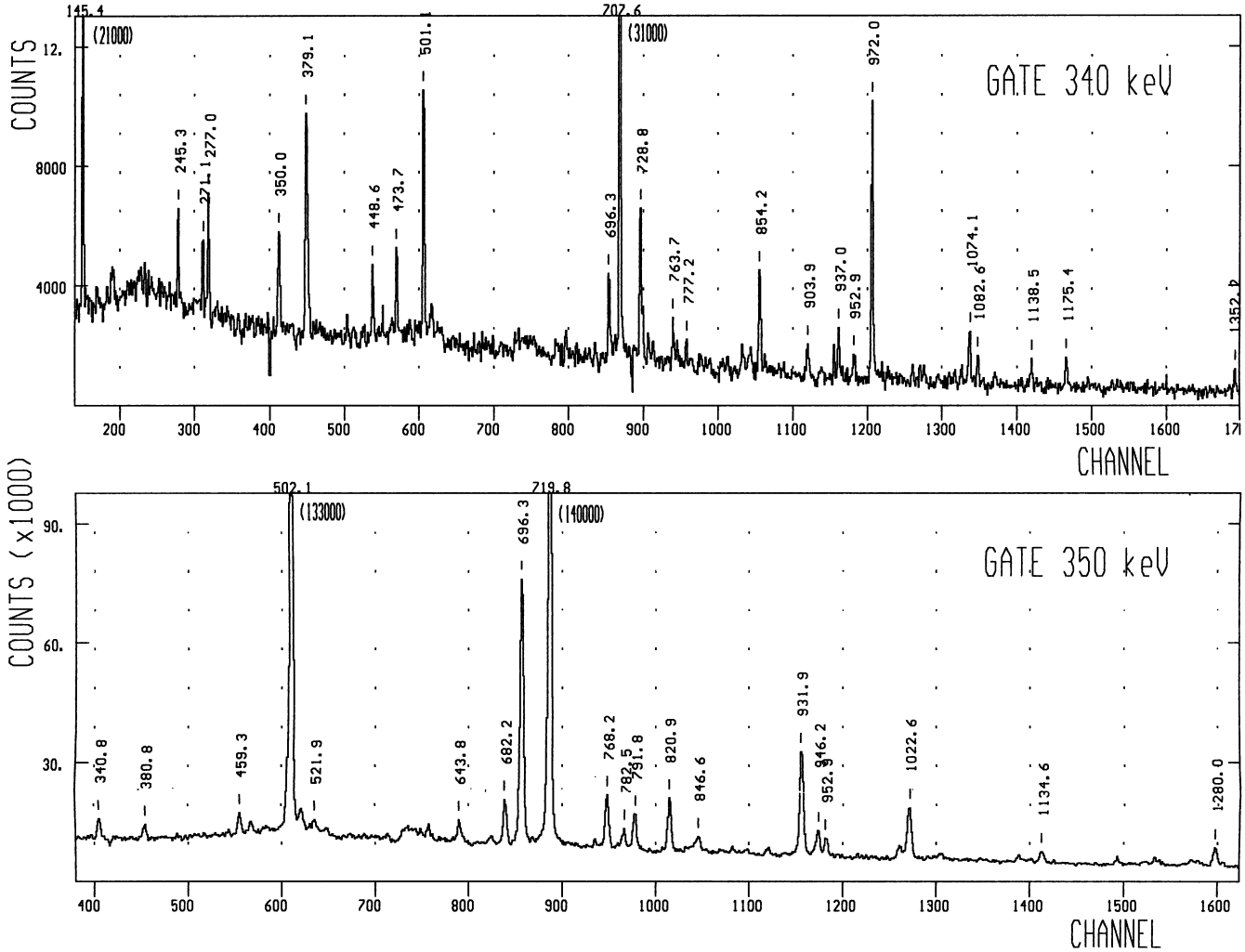

Fig. 2. Coincident spectra, corrected for the background in the gate

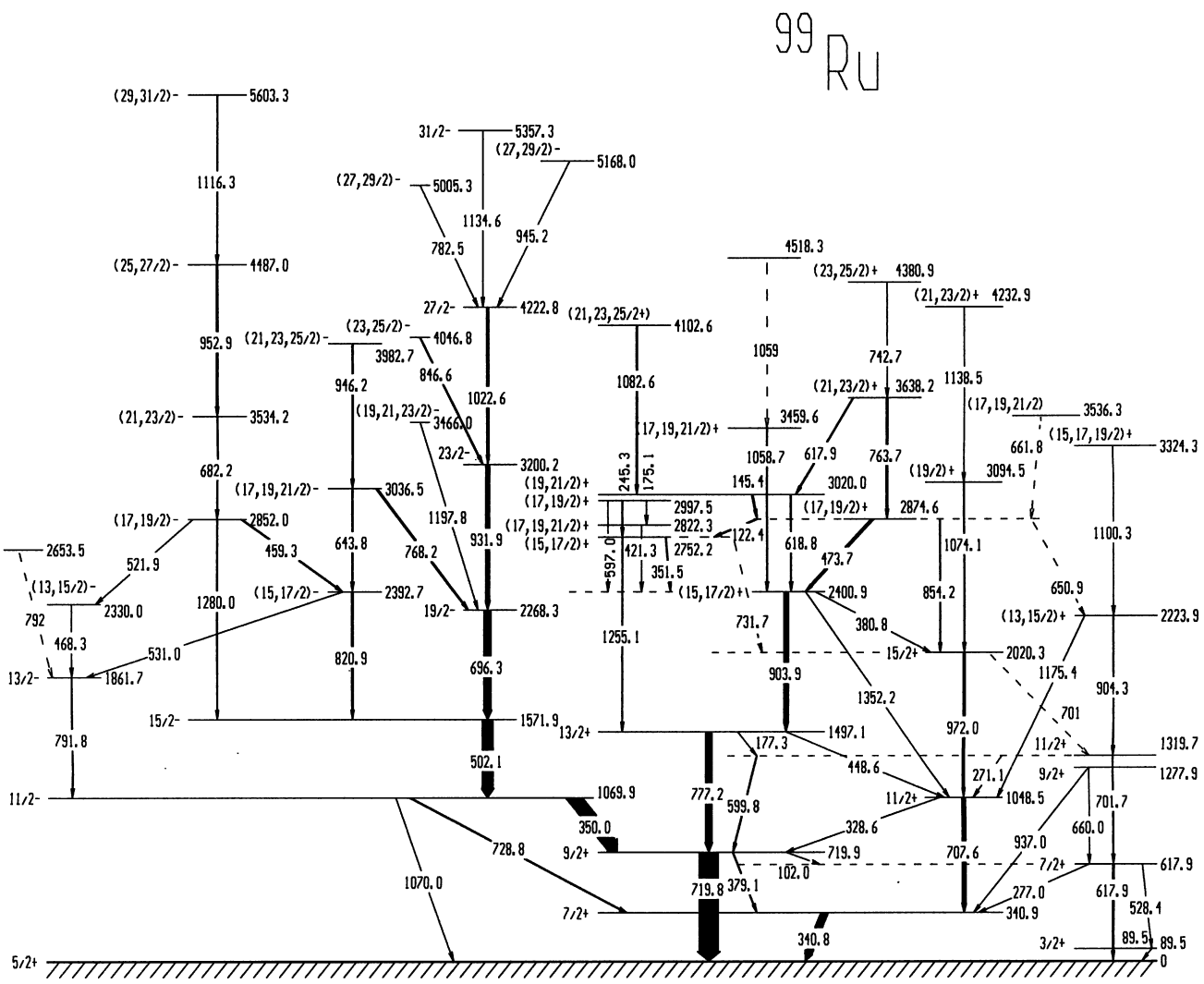

Fig. 3. Scheme of the ^{99}Ru excited states from the present work

lineshape analysis, was used for lifetime values extraction from the γ–ray spectra.

The SHAPE uses the statistical theory of nuclear reactions to describe an excited states feeding in a produced nucleus. Monte–Carlo simulation is employed to model kinematics. LSS (Lindhard-Scharff-Schiott) theory, with correction factors for nuclear and electron stopping power parts, obtained in a half–thick target experiment [18], is used to model slowing down processes in a target.

4 Results

Results obtained from angular distribution measurements are presented in Table 1. The table contains transition energies, relative γ–ray intensities, angular distribution coefficients a_2 and a_4, expected spin and parity of initial I_i and final I_f levels and mixing ratio δ for transitions of mixed multipolarity.

The level scheme was built up from our γ–γ coincidence data with the aid of previous works [7,13–15], which established the low–lying levels and their decay properties. The level scheme is presented in Fig. 3.

4.1 A part of the scheme above $11/2^-$ state at 1069.9 keV

Changes in part of the scheme with expected negative parity states were proposed. The transition sequence 682.2, 952.9 and 1116.3 keV feeding the 1571.9 keV level ([14]) was moved above the newly observed level at energy 2852.0 keV. New levels at 2330.0, 3466.0, 4046.8 and 5005.3 keV were observed. Introduction of a 792 keV transition deexciting the 2653.5 keV level is based on observed coincidences of the 792 keV peak with itself, so its proper placement is uncertain. Our suggested placement is based on a coincidence intensity comparison. Moreover, an E3 transition of 1070.0 keV to the ground state was observed

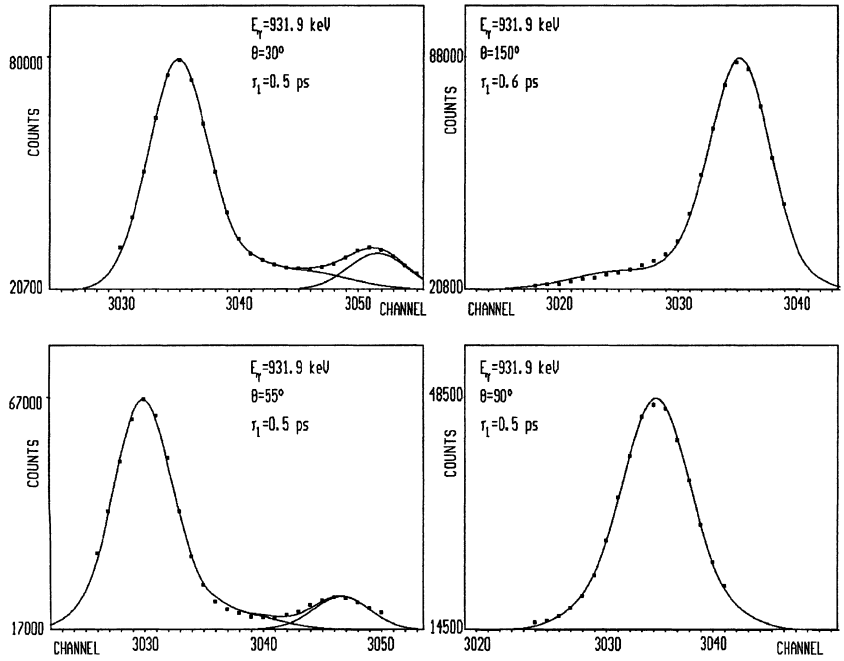

Fig. 4. Examples of experimental spectra of 931.9 keV transition influenced by Doppler effect and fitted lineshape based on DSA method. Detector was placed at θ degrees to the beam axis

in coincidences with the 502.1, 696.3 and 931.9 keV transitions. Its relatively high B(E3)[1] value of 3.5 ± 2.2 W.u.[2] points on a probable role of coupling the octupole vibration with the $d_{5/2}$ single particle state giving rise to the level at 1069.9 keV [20].

4.2 A part of the scheme above the $7/2^+$ and $9/2^+$ levels

A rather complicated situation was found in part of the scheme with supposed positive parity levels. The presence of a 903.9, 904.3 keV doublet found in [15] was confirmed and the existence of the 2223.9 keV level was confirmed by observation of the deexciting 1175.4 keV transition.

Spin and parity $17/2^+$ was suggested for the level at 2400.9 keV in previous works [14,15]. The 1352.2 keV transition feeding the 1048.5 keV level was found in the coincidences. The energy of its initial level is close to 2400.9 keV, but the coincidences did not give an unambiguous answer about the initial level identity. In case of spin 17/2 of its initial level, the 1352.2 keV transition has multipolarity M3, which is unlikely, because of the B(M3)[3] value in the order of 10^6 W.u. Thus either the 1352.2 keV transition deexcites a new level, which is close in energy to the 17/2 one, or the initial level spin must be less then 17/2, which would mean major changes in the ^{99}Ru structure.

The transition of 177.3 keV was observed in coincidences with the 599.8 keV transition, but not with the 701.7 keV transition. No coincidences of the 177.3 keV transition were observed in previous works [21,15].

The newly observed levels at 3094.5 keV and 4232.9 keV are candidates for possible continuation of the $11/2^+$, $15/2^+$ rotational band sequence crossed by a sideband. Furthermore, new levels at 2752.2, 2822.3 and 2997.5 keV based on coincidences of transitions 1255.1, 597.0, 245.3, 421.3, 175.1 and 351.5 keV were observed.

The 1082.6 keV transition was placed above the 3020.0 keV level. A more complicated coincidence spectrum was observed for transition 1082.6 keV, but the origin of these coincidences is uncertain. These coincidences either originate from the higher part of the scheme or the 1082.6 keV peak has an unresolved component. The observed coincidences of 1082.6 keV with new transitions of 1255.1 and 245.3 keV can be explained by assuming the existence of 22.5 keV multipolarity M1 transition deexciting the 3020.0 keV level.

A new level at 4380.9 keV deexcited by the 742.7 keV transition was introduced. A cascade of two $\sim$ 1059 keV transitions was suggested from coincidence data, coincidences 1059–1059 were observed and coincidences 473.7–1059 of about eight times lower intensity in comparison with 1059–903.9 coincidence intensity.

Values of a previously deduced and present mixing ratios δ were compared. All values are in agreement within 2σ interval, except for the 328.6 keV transition value, which was found in 3σ interval.

4.3 Level lifetimes

The lifetimes of ^{99}Ru levels determined by the DSA method mentioned in Subsect. 3.2 are shown in Table 2. All data are new except of the 3036.5 keV level lifetime. The calculated B(E2) values are shown in Table 3.

[1] The lifetime of 1069.9 keV level is taken from [19]

[2] Reduced transition probability in Weisskopf units: 1 W.u.(M1) = $1.79\mu_N^2$, 1 W.u.(E2) = $2.7210^{-3}e^2b^2$, 1 W.u.(M3) = $7.6\ 10^{-2}\mu_N^2b^2$, 1 W.u.(E3) = $5.88\ 10^{-4}e^2b^3$

[3] The lifetime of 2400.9 keV level is taken from [19].

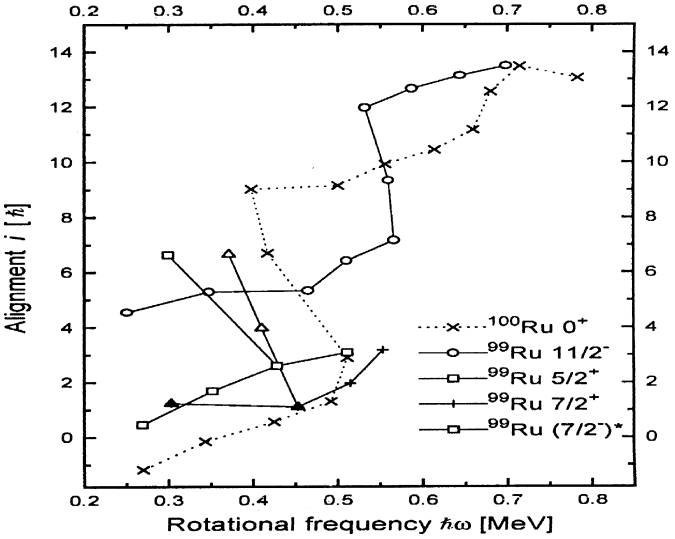

Fig. 5. Plots of aligned angular momentum (i_x) vs. $\hbar\omega$ for bands in ^{99}Ru and ^{100}Ru. See text for more details

Table 2. Mean lifetimes of ^{99}Ru levels

E_{lev} [keV]	E_γ [keV]	τ [ps]
3036.5[a]	643.8	$0.6^{+0.2}_{-0.1}$
	768.2	$0.8^{+0.2}_{-0.1}$
3094.5	1074.1	$0.6^{+0.5}_{-0.25}$
3200.2	931.9	$0.5^{+0.2}_{-0.1}$
3466.0	1197.8	$0.8^{+0.4}_{-0.2}$
3982.7	946.2	> 1.3
4102.6[b]	1082.6	$1.0^{+0.2}_{-0.2}$
4222.8	1022.6	$0.85^{+0.1}_{-0.1}$
4232.9	1138.5	$1^{+3}_{-0.5}$
4487.0	952.9	$0.6^{+0.2}_{-0.2}$
5168.0	945.2	$0.3^{+0.2}_{-0.1}$
5357.3	1134.6	$0.4^{+0.2}_{-0.1}$
5603.3	1116.3	$0.3 \div 1$

[a] accepted value $\tau = 0.7^{+0.2}_{-0.1}$ ps

[b] probable doublet or possible undetermined influence of complex scheme

The lifetime value of 0.35 ± 0.14 ps of the 3036.5 keV level measured by Doinikov et al. [22] was rectified by Pasternak et al. [23] to 0.5 ± 0.2 ps. Our result ($0.7^{+0.2}_{-0.1}$ ps) is in better agreement with the latter value [23].

An example of a part of experimental spectrum and fitted lineshape obtained from the program package SHAPE is presented in Fig. 4.

5 Aligned angular momentum analysis

New information about the structure of ^{99}Ru were analysed in angular momentum plots.

Following the prescription of Bengtsson and Frauendorf [24] Fig. 5 shows plots of the aligned angular momentum corrected for collective rotation (i_x) as a function of rotational frequency ($\hbar\omega$). The parameters for the collective reference band, J_0=8.9 $\hbar^2 MeV^{-1}$ and J_1=15.7 $\hbar^4 MeV^{-3}$, and high spin data for ^{99}Ru and ^{100}Ru were taken from the work of Gizon et al. [7].

Plots for bands above the $5/2^+$ state (transitions 719.8 – 777.2 – 903.9 – 618.8 and/or 1058.7 keV) and the $7/2^+$ state (transitions 707.6 – 972.0 – 854.2 – 763.7 keV) are drawn with the assumption of stretched E2 nature of the 903.9 keV transition.

New levels 3094.5, 4232.9 keV deexcited by transitions 1074.1 and 1138.5 keV form with 1048.5 and 2020.3 keV levels a band above $7/2^+$ (transitions 707.6 – 972.0 – 1074.1 – 1138.5 keV), here marked as $7/2^+*$.

Table 3. Reduced transition probabilities B(σ L) in ^{99}Ru

E_γ[keV]	I_i^π	I_f^π	σL	$B(\sigma L)$ [W.u.]
643.8	$(21/2^-)$	$(17/2^-)$	E2	110^{+25}_{-30}
	$(19/2^-)$	$(17/2^-)$	M1	$0.037^{+0.013}_{-0.012}$ [a]
	$(19/2^-)$	$(17/2^-)$	E2	24^{+15}_{-11} [a]
	$(17/2^-)$	$(17/2^-)$	M1	$0.046^{+0.013}_{-0.015}$
	$(17/2^-)$	$(17/2^-)$	E2	5^{+11}_{-5}
768.2	$(21/2^-)$	$19/2^-$	M1	$0.053^{+0.016}_{-0.019}$ [a]
	$(21/2^-)$	$19/2^-$	E2	30^{+21}_{-13} [a]
	$(17/2^-)$	$19/2^-$	M1	$0.036^{+0.028}_{-0.018}$
	$(17/2^-)$	$19/2^-$	E2	60^{+30}_{-40}
1074.1	$(19/2^+)$	$15/2^+$	E2	35^{+25}_{-16}
	$(17/2^+)$	$15/2^+$	M1	$0.04^{+0.028}_{-0.022}$ [a]
	$(17/2^+)$	$15/2^+$	E2	5^{+10}_{-4} [a]
931.9	$23/2^-$	$19/2^-$	E2	85^{+20}_{-25}
1197.8	$(23/2^-)$	$19/2^-$	E2	15 ± 5
	$(21/2^-)$	$19/2^-$	M1	$0.017^{+0.007}_{-0.008}$ [a]
	$(21/2^-)$	$19/2^-$	E2	$4^{+4}_{-1.9}$ [a]
946.2	$(25/2^-)$	$(21/2^-)$	E2	< 30
	$(23/2^-)$	$(21/2^-)$	M1	< 0.24
	$(23/2^-)$	$(21/2^-)$	E2	< 6.64 [a]
	$(21/2^-)$	$(21/2^-)$	M1	< 0.029
	$(21/2^-)$	$(21/2^-)$	E2	< 4.18
1082.6[b]	$(25/2^+)$	$(21/2^+)$	E2	20^{+5}_{-3}
	$(23/2^+)$	$(21/2^+)$	M1	$0.022^{+0.006}_{-0.005}$ [a]
	$(23/2^+)$	$(21/2^+)$	E2	$2.8^{+1.7}_{-1.2}$ [a]
	$(21/2^+)$	$(21/2^+)$	M1	$0.013 \div 0.032$
	$(21/2^+)$	$(21/2^+)$	E2	< 10
1022.6	$27/2^-$	$23/2^-$	E2	31 ± 5
1138.5	$(23/2^+)$	$(19/2^+)$	E2	16^{+15}_{-12}
	$(21/2^+)$	$(19/2^+)$	M1	$0.019^{+0.023}_{-0.016}$
	$(21/2^+)$	$(19/2^+)$	E2	$2^{+9}_{-1.9}$
952.9	$(27/2^-)$	$(23/2^-)$	E2	60^{+35}_{-15}
945.2	$(29/2^-)$	$27/2^-$	M1	$0.10^{+0.07}_{-0.06}$ [a]
	$(29/2^-)$	$27/2^-$	E2	30^{+60}_{-22} [a]
	$(27/2^-)$	$27/2^-$	M1	$0.12^{+0.07}_{-0.07}$
	$(27/2^-)$	$27/2^-$	E2	< 58
1134.6	$31/2^-$	$27/2^-$	E2	40 ± 15
1116.3	$(31/2^-)$	$(27/2^-)$	E2	$17 \div 57$

[a] if two values δ are found, the less one is used for B(σ L) evaluation (see Table 1)

[b] probable doublet or possible undetermined influence of complex scheme

The band (transitions 707.6 – 972.0 – 854.2 – 763.7 keV), which is after bandcrossing likely based on a $h_{11/2}$ aligned neutron pair coupled to a $g_{7/2}$ neutron, is marked as $7/2^+$.

The experimental aligned angular momentum seems to indicate a $\nu h_{11/2}$ origin for bandcrossing in ^{100}Ru at $\hbar\omega \sim 0.46$ MeV [7,9] and bandcrossing in $11/2^-$ band of ^{99}Ru at $\hbar\omega \sim 0.56$ MeV is assigned to a $\pi g_{9/2}$ pair [7]. Our supplementary data on $7/2^+$ band of ^{99}Ru (Fig. 5) and $5/2^+$ and $7/2^+$ bands of ^{101}Ru (published in [10]) support the $\nu h_{11/2}$ explanation.

New data for the $7/2^+*$ band show a possible start of bandcrossing at $\hbar\omega \sim 0.7$ MeV similar to the effect observed in $9/2^+$ band of ^{103}Rh (based on $g_{9/2}$ proton state), where the other probable backbending origins coming into account are $\nu d_{5/2}$ and $\nu g_{7/2}$. If those two effects have the same origin, the $\nu d_{5/2}$ pair may play a role in this upband.

6 Conclusion

Changes and extensions to the level scheme of ^{99}Ru were proposed, new data about angular distribution coefficients and mixing ratios δ were presented. Lifetimes of eleven higher spin states were deduced by DSA method. Spin alignment was studied and possible role of $d_{5/2}$ neutron pair was accentuated.

We are grateful to the cyclotrone machine staff whose outstanding efforts made possible this experiment.

References

1. Troltenier, D., Maruhn, J.A., Greiner, W., Aguilar, Velasquez V., Hess, P.O., Hamilton, J.H.: Z. Phys. A**338**, 261 (1991)
2. Bharti, A., Khosa, S.K.: Nucl. Phys. A**572**, 317 (1994)
3. Bucurescu, D., Cata, G., Cutoiu, D., Constantinescu, G., Ivascu, M., Zamfir, N.V.: Z. Phys. A**324**, 387 (1986)
4. Stachel, J., Van Isacker, P., Heyde, K.: Phys. Rev. C**25**, 650 (1982)
5. Frank, A., Van Isacker, P., Warner, P.D.: Phys. Lett. **197B**, 474 (1987); A.Frank: Phys. Rev. C**39**, 652 (1989)
6. Mrázek, J.: Dissertation work, MFF UK Prague 1998
7. Gizon, J., Jerrestam, D., Gizon, A., Jozsa, M., Bark, R., Fogelberg, B., Ideguchi, E., Klamra, W., Lindblad, T., Mitarai, S., Nyberg, J., Piiparinen, M., Sletten, G.: Z. Phys. A**345**, 335 (1993)
8. Bengtsson, R., Bengtsson, T., Dudek, J., Leander, G., Nazarewicz, W., Zhang, J.-Y.: Phys. Lett **183B**, 183 (1987)
9. Haenni, D.R., Dejbakhsh, H., Schmitt, R.P., Mouchaty, G.: Phys. Rev. C**333**, 1543 (1986)
10. Mrázek, J., Honusek, M., Špalek, A., Bielčík, J., Slívová, J., Pasternak, A.A.: Acta Phys. Polonica B**29**, 433 (1998)
11. Frána, J.: Acta Polytechnica Vol. 38 No. 3, 127 (1998)
12. Hamilton, W.D.: The Electromagnetic Interaction in Nuclear Spectroscopy, Amsterdam, Oxford: North-Holland Publ. Comp. 1975
13. Lederer, C.M., Jaklevic, J.M., Hollander, J.M.: Nucl. Phys. A**169**, 489 (1971)
14. Du Marchie Van Voorthuysen, E.H., De Voigt, M.J.A., Blasi, N., Jansen, J.F.W.: Nucl. Phys. A**355**, 93 (1981)
15. Whisnant, C.S., Carnes, K.D., Castain, R.H., Rickey, F.A., Samudra, G.S., Simms, P.C.: Phys. Rev. C**34**, 443 (1986)
16. Lemberg, I.Ch., Pasternak, A.A.: Sovremennyje metody jadernoj spektroskopii 1984. Nauka, 3 Moskva 1985
17. Pasternak, A.A.: Programs for lifetime evaluation by DSA method, priv. comm.
18. Kudojarov, M.F., Kuzmin, E.V., Pasternak, A.A., Honusek, .M., Špalek, A., Adam, I., Kult, K.: Abstracts of the Conference on Nucl. Spectroscopy and Structure, p. 59, Alma–Ata 1992
19. Peker, L.K.: Nuclear Data Sheets **73**, 1 (1994)
20. Ejiri, H., de Voigt, M.J.A.: Gamma–Ray and Electron Spectroscopy in Nuclear Physics, Oxford: Clarendon press 1989
21. Kajrys, G., Lecomte, R., Landsberger, S., Monaro, S.: Phys. Rev. C**28**, 1504 (1983)
22. Doinikov, D.N., Erokhina, K.I., Efimov, A.D., Zhovliev, U.I., Kudoyarov, M.F., Pasternak, A.A.: Izv. Akad. Nauk SSSR, Ser. Fiz. **51**, 194
23. Pasternak, A.A., Kudoyarov, M.F., Rassadin, L.A., Zhovliev, U.J.: Program and Theses. Proc. 37th Ann. Conf. Nucl. Spectrosc. Struct. At. Nuclei, Yurmala, 72 (1987)
24. Bengtsson, R., Frauendorf, S.: Nucl. Phys. A**327**, 139 (1979)